Chapter

Advantages of Digital Technology in the Assessment of Bone Marrow Involvement by Magnetic Resonance Images

Pilar Giraldo Castellano and Mercedes Roca Espiau

Abstract

Magnetic resonance imaging (MRI) is the gold standard for evaluating bone marrow (BM). The information provided is a useful tool for obtaining a global map of the contents of the medullary cavity. The applications of this technique to the study of different processes affecting the bone marrow are of great importance to know the extension of disease, to distinguish by image different entities, and to evaluate response to therapies. Actually, machine learning tools aid in the interpretation of images and patterns that are not visible or are unfamiliar to the observer. In addition, integrating clinical, biological, and therapeutic data with imaging using artificial intelligence methods applied to these studies provides a broad perspective and tool that can predict the risk of complications. The systematic inclusion of structured bone marrow MRI reporting is useful to standardize the collected data collaborate in developed algorithms to learning model, and facilitate clinical management and academics collaboration.

Keywords: bone marrow, MRI, infiltration patterns, lysosomal disorders, structured reports, machine learning

1. Introduction

This chapter reviews the information provided by magnetic resonance imaging (MRI) as a useful tool to obtain a global map of the content of the medullary cavity and the applications of the technique to the study of different processes affecting bone marrow.

The daily clinical practice involves resolving situations of uncertainty in order to obtain the most accurate diagnosis possible and initiate therapeutic measures quickly. In this sense, the exchange of information and collaboration between the clinical physician and the MRI specialist is essential to answer questions regarding the global or focal involvement of the bone marrow in various pathological situations.

MRI, as a useful imaging technique to distinguish differences and anomalies in different tissues, bases its resolution on reflecting the balance between the medullary

fatty component and the hematopoietic cellular component, providing an image of the variations that occur between these components within the bone cavity [1].

Artificial intelligence (AI) models based on deep learning algorithms offer actually diagnostic assessment and follow-up assistance for low-frequency entities, with findings to date suggesting that the diagnostic performance of such systems is equivalent to that of health-care professionals [2].

2. Rational basis of magnetic resonance imaging

The physical basis of the procedure is due to the property possessed by some atomic nuclei of orientation in a magnetic field and the emission of a signal when subjected to an electromagnetic wave of an appropriate frequency. The basis is sending a sound signal on a magnetized object, developing macroscopic magnetization phases, which disturb the state of equilibrium due to the sound signal and collection of the MR signal and the return to the state of equilibrium or relaxation. This signal of a return to equilibrium or relaxation is the MR signal [3].

Some notions to keep in mind are the following:

- The relaxation phenomenon characterizes the times T1 and T2.
- The repetition time or TR is the interval that separates 2 impulses/2 successive.
- The echo time or TE is the time interval separating the impulse/2 from the measurement of the emitted signal.
- The longitudinal relaxation time or T1 represents the growth of the magnetism M (Mz component) to return to its initial value. It is an exponential growth, which takes place slowly.
- The transverse relaxation time or T2 represents the decrease of the vector M (Mxy component) to return to its initial value. It occurs rapidly and is linked to the loss of proton coherence.
- T1-weighted sequences provide information on anatomical landmarks, and T2 sequences provide a closer approximation to the histological characterization of the involvement.
- The STIR sequence adds a fat suppression effect and chemical shift artifact elimination. It combines a short T1 with a long TR and shows a contrast between healthy and pathologic tissue superior to conventional T2.
- In phase-out-of-phase: Due to its lack of proton content, the trabecular bone does not present an MR signal but creates heterogeneities in the magnetic field. This is more evident in Gradient echo sequences where this artifact can be contributory. Therefore, if the trabeculae have been destroyed, the artifact is smaller, and the signal intensity will be higher.
- Diffusion-weighted MR imaging (DWI) is a technique that assesses motion of watermolecules in the soft tissues, known as Brownian motion, for tissue

characterization. A DWI sequence may be helpful for lesion detection, but its utility in evaluating and characterizing focal bone marrow lesions is unknown. MR Spectroscopy. MRS is useful for fat quantification, and bone marrow studies have primarily focused on its use in the imaging of osteoporosis [4].

3. Applications of magnetic resonance imaging to the study of bone marrow

In general, bone marrow involvement is easy to detect and interpret by MRI without requiring sophisticated sequences; it is very useful to obtain a map of hematopoietic marrow distribution and infiltration.

3.1 Normal bone marrow distribution

In children, bone marrow occupies 85% of the bone and accounts for 5% of the body weight. In the adult, red marrow is located in vertebrae, sternum, ribs, epiphyses of long bones, and iliac crests.

The bone marrow content in adults is 70% water and 30% fat. Hematopoietic marrow (red) consists of 40% water, 40% fat, and 20% protein. The fatty marrow (yellow) is made up of 15% water, 85% fat, and 5% protein.

Normal bone always contains both fat and red marrow, the percentage depending on age and anatomical region (**Figure 1**). However, it undergoes variations in its fatty composition/hematopoietic cellularity as part of a transformation phenomenon and in dependence on cellular requirements. Fat tissue is very labile and can be replaced by hematopoietic tissue under the influence of appropriate stimuli. Anatomically,

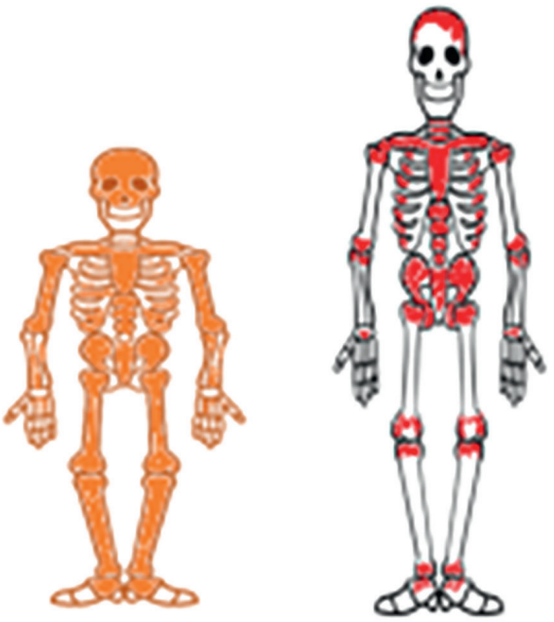

Figure 1.
Distribution of red marrow and fat. A in the child. Red bone marrow is distributed in 85% of the bones. B in the adult, the red bone marrow is located in vertebrae, sternum, ribs, epiphyses of long bones, and iliac crests.

medullary repopulation occurs in the reverse direction of regression, i.e., from proximal to distal areas.

MRI is able to reflect the ratio between the medullary fatty and hematopoietic components, through the changes that occur within the bone cavity [5, 6].

Marrow fat has a signal analogous to subcutaneous fat, the signal intensity is high due to its high proton content, expressing itself with a short T1 and a long T2 with high signal intensity in T1 and T2. As we have said, normal bone marrow contains 70% water and 30% fat and is hypointense in T1 and T2. T1 is the fundamental sequence for the study of bone marrow. The bone cortex has low proton content and small signal intensity.

Fat has a high signal in T1 and T2. Red marrow has an intermediate signal lower than fat and higher than muscle. The alterations that can occur are reconversion, infiltration, depletion, edema, and ischemia [7].

3.2 Patterns of bone marrow infiltration by MRI

The distribution of bone marrow involvement may be diffuse or focal. Several distribution patterns have been described according to the images that appear on magnetic resonance imaging. **Table 1** shows the patterns described by Moulopoulos et al. [8] in the study of the bone marrow in patients with bone marrow involvement and the one described by our group [9] (**Figure 2**).

3.3 Hematological entities with preferential involvement of bone marrow

3.3.1 Multiple myeloma (MM)

Eighty percent of patients with multiple myeloma present osteolytic lesions or demineralization at the time of diagnosis [10]. When these lesions become evident on radiography, more than 50% of the bone is already occupied.

There are three described patterns of infiltration in MM by MRI [11]:

1. Focal lesions, associated with lytic lesions in radiology, are the most frequent (**Figure 2**).

2. Diffuse infiltration appears in 25% of patients and is associated with decreased hemoglobin and a high percentage of medullary plasmacytosis. The MR signal is hypointense in T1 with diffuse gadolinium uptake (**Figure 3**).

According to Moulopoulos et al. [8]	**According to Roca et al.** [9]
Focal	Homogeneous (H)
Variegated (or variegata)	Nonhomogeneous (NH):
Diffuse	reticular (NHR)
	mottled (NHM)
	diffuse (NHD)

Table 1.
Patterns of bone marrow infiltration by MRI.

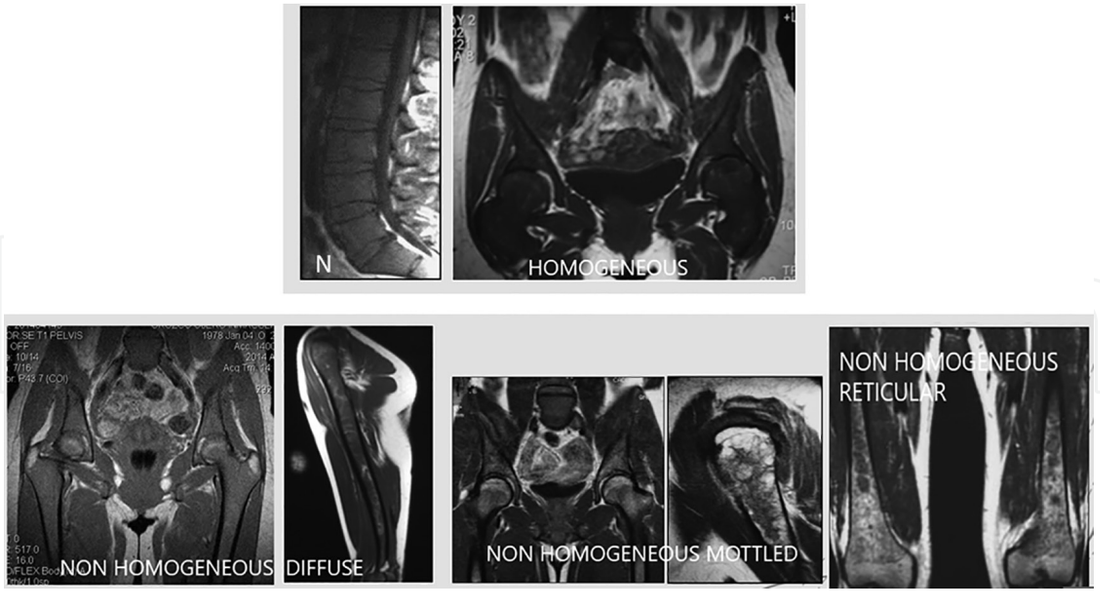

Figure 2.
Bone marrow infiltration. MRI patterns described by Roca-Espiau et al. 2007. Three MRI patterns were defined: Normal, homogeneous, and nonhomogeneous infiltration subtypes reticular, mottled, and diffuse.

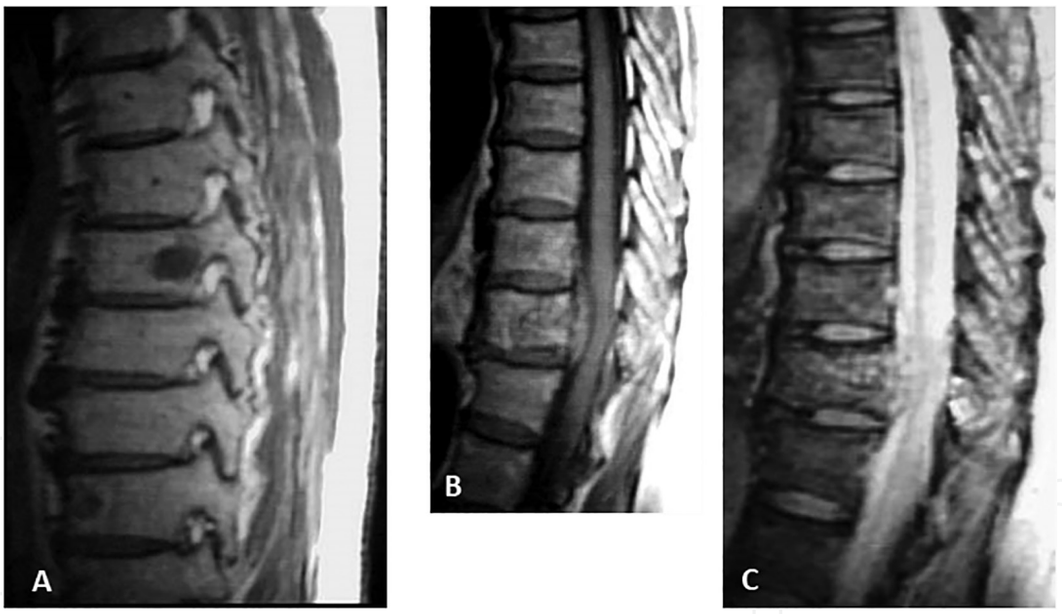

Figure 3.
Sagital spin echo (SE) T1 (A) focal pattern in spine in multiple myeloma. It is the most frequent lesions and corresponds to lytic images in plain radiology. SE T1 (B) and T2 (C) spine with diffuse infiltration. The MR signal is hypointense in T1.

3. Mottled or variegated pattern, with hypointense foci in T1 and generally hyperintense in T2 and STIR with contrast uptake (**Figure 4**). Libshitz et al. [12] describe diffuse involvement as areas where myeloma cells mix with hematopoietic cells, producing a displacement of hematopoiesis caused by nodular accumulations formed mainly by plasma cells. For this reason, the appearance of MRI is variable.

A strong association between diffuse infiltration and disease progression has been described. Diffuse infiltration is an unfavorable prognostic factor in patients with

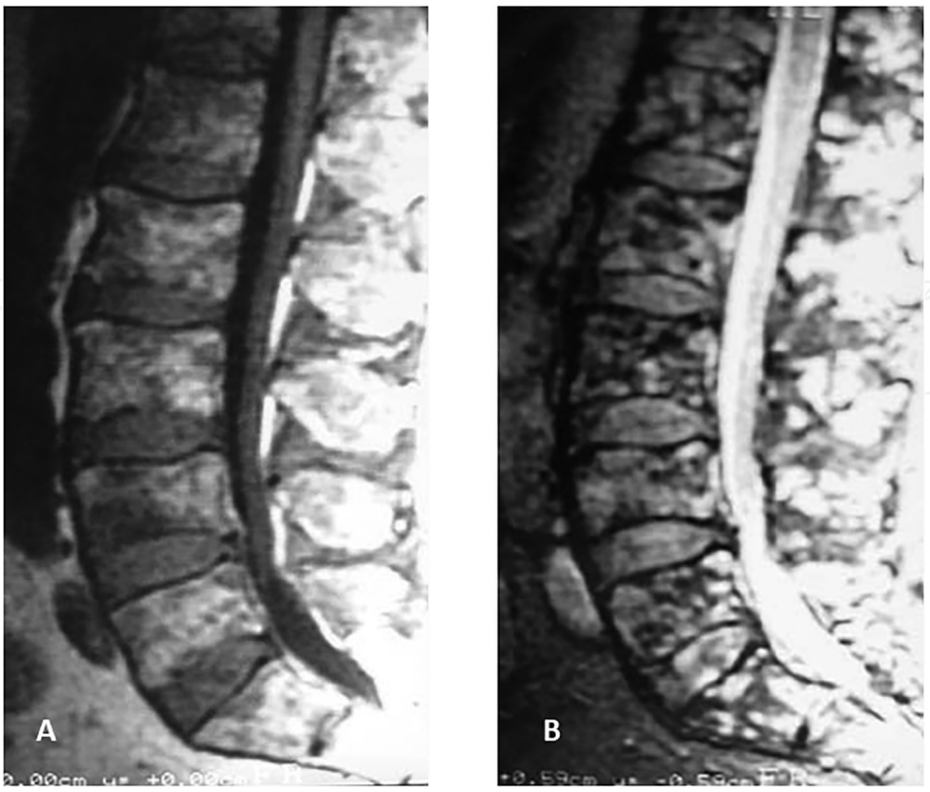

Figure 4.
Sagital spin echo (SE) T1 (A) and T2 (B) mottled or variegated pattern in multiple myeloma, with hypointense foci in T1 and hyperintense in T2.

normal bone radiology [13]. Approximately 15% of patients are asymptomatic at the time of diagnosis, but bone marrow infiltration can already be detected in up to 29–50% of patients [11–14]. Patients with focal and diffuse MR patterns tend to progress more rapidly than patients with mottled patterns. Following these criteria, MR infiltration imaging helps to identify patients who are at higher risk of complications and to predict disease progression [15, 16]. However, in the current diagnostic criteria for MM, only the focal pattern on MRI (> 1) is considered as a criterion for multiple myeloma (previously called symptomatic myeloma) and, therefore, an indication for treatment [16, 17].

MRI is probably not the most sensitive imaging procedure in the follow-up of the response in MM, since bone lesions will persist over time, and it is not possible to delimit whether it is an active lesion. It is, however, useful for comparative assessment of lesion progression [18, 19].

In the variety of light chain multiple myeloma, a different MRI pattern of mottled appearance with hypointense foci in both T1 and T2 have been described, analogous to the pattern that appears in Gaucher disease [20]. The diagnosis of solitary plasmacytoma requires histologic demonstration of plasma cell infiltration. Although radiotherapy can eradicate this lesion, most patients progress to multiple myeloma, which has been attributed to occult disease growth [21].

For this reason, MRI is important in the extension study, since it detects unsuspected lesions, especially at the vertebral level. Currently, the accepted treatment for these lesions is radiotherapy covering at least 2 cm outside the tumor, and for this purpose, it is recommended to perform a previous MRI of the plasmacytoma area.

The consensus panel (International Myeloma Workshop 2011) [22] recommends MRI in three situations:

- Asymptomatic myeloma (smoldering myeloma) to detect occult lesions.
- In symptomatic, for visualization of unsuspected focal lesions and soft tissue plasmacytomas in the spine and pelvis.
- In symptomatic, to predict evolution, according to the MRI pattern.

3.3.2 Non-Hodgkin's lymphoma and Hodgkin's lymphoma

Bone marrow infiltration occurs in 5–15% of patients with Hodgkin's lymphoma and in 25–40% of patients diagnosed with non-Hodgkin's lymphoma. In T1, the pattern of involvement is heterogeneous diffuse, with focal infiltration being less frequent. In T2, hypersignal is observed, as well as contrast uptake after gadolinium injection. This aspect is nonspecific and indistinguishable from other spinal cord infiltration of other origins, and there is no difference in the MRI pattern between the different histological types of lymphoma [23, 24] (**Figure 5**).

Due to the permeative nature of lymphomas, tumor extension can be observed in the form of a soft tissue mass without rupture of the bone cortex. Although it is not pathognomonic, since it can exist in other malignant lesions, especially in small cell tumors, its detection, and evaluation with MRI is highly suggestive of lymphoma [25].

3.3.3 Chronic myeloproliferative neoplasms

3.3.3.1 Polycythemia vera

In polycythemia rubra vera, the bone marrow of the axial skeleton appears hypointense in T1 with a diffuse and homogeneous character in MRI studies, being

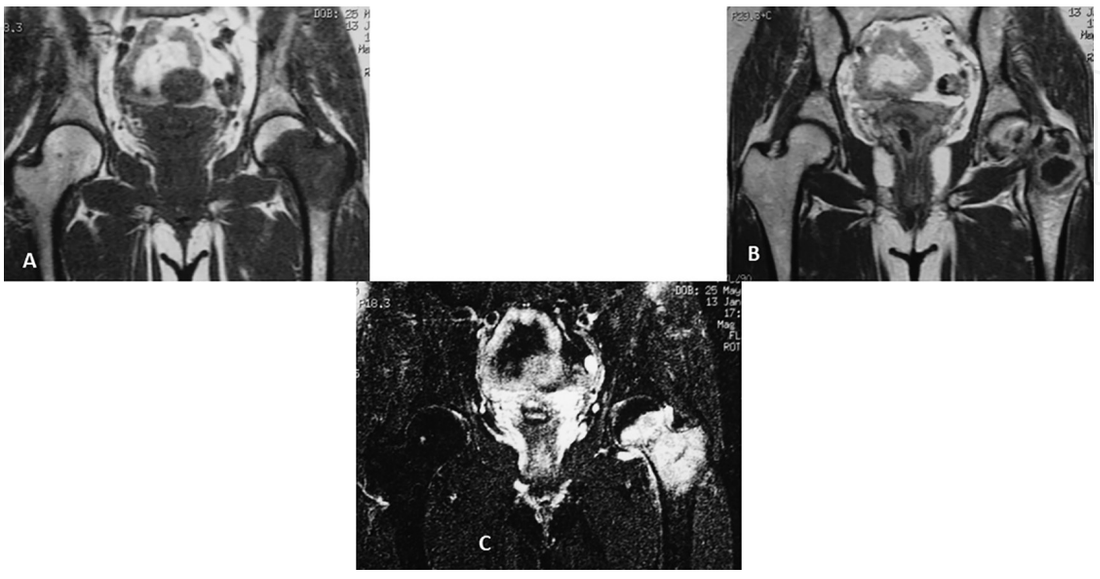

Figure 5.
Coronal pelvis spin echo (SE) T1 (A), T1 Gadolinio (B), and T2 FSat (C) in non-Hodgkin lymphoma. Pattern heterogeneous diffuse in T1, hyperintensity of signal in T2, contrast uptake after gadolinium injection.

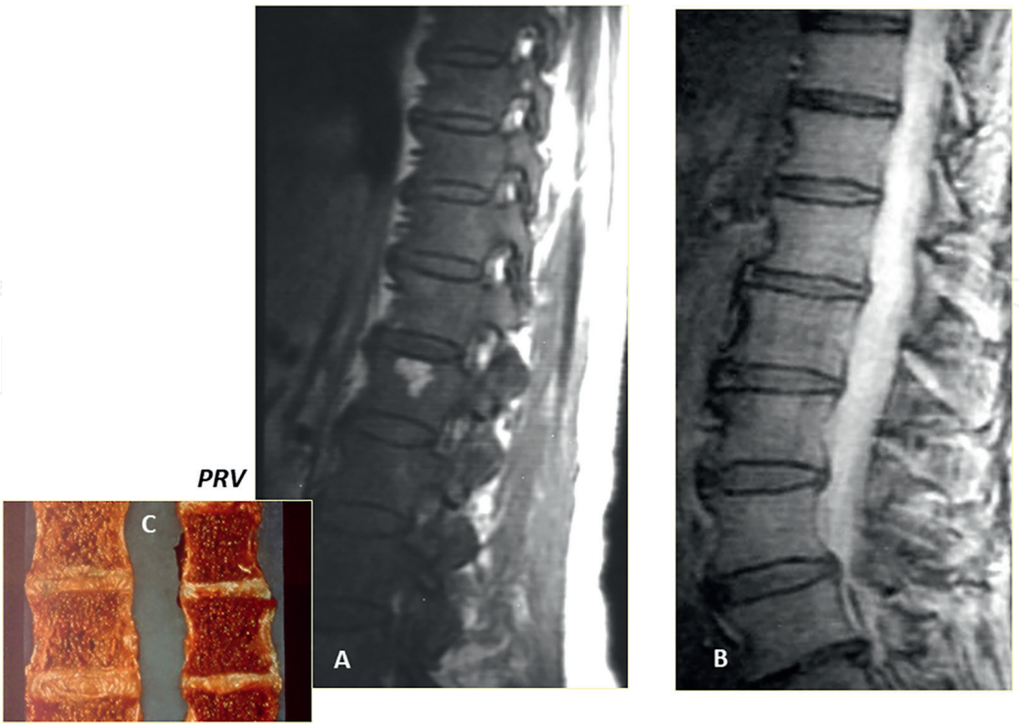

Figure 6.
Sagital spin echo (SE) T1 (A) and T2 (B) diffuse pattern in chronic myeloproliferative neoplasia (polycythemia rubra vera (PRV)). (C) Macroscopic section of spine with red infiltration PRV (right image) versus normal (left image).

indistinguishable from the diffuse involvement observed in other myeloproliferative neoplasia. When the reconversion is pronounced, the proximal epiphyses of the femur and humerus and the greater trochanter, also participate in the reconversion showing hyposignal in T1. In T2, the behavior can be variable depending on the cellularity, the extent of reticulin fibrosis, and the paramagnetic effect of iron if hemosiderosis is present (**Figure 6**). The assessment in the proximal femur can be quantified according to the involvement of the femoral head and greater trochanter. The greater trochanter is more resistant to reconversion than the epiphyses. Patients with infiltration of both have higher disease activity [26, 27].

3.3.3.2 Myelofibrosis

The fibrotic medulla, typical of primary or secondary myelofibrosis, is visualized in MRI as low signal areas in all sequences, but its appearance is nonspecific as in the rest of hematologic diseases and does not differentiate primary from secondary myelofibrosis. There is usually contrast uptake due to increased capillaries, large sinusoids, and increased vascular permeability [28]. Our group has performed a comparative study in patients diagnosed with primary or secondary myelofibrosis between histological findings and the pattern of bone marrow involvement by MRI. The results showed that the bone marrow patterns defined from lesser to a greater degree of involvement were: normal patterns according to age (NP), hematopoietic hyperplasia (HHP), reticular infiltration pattern (RP), mottled infiltration pattern (MP), diffuse heterogeneous infiltration pattern (DHI) and diffuse homogeneous infiltration pattern (HP) [29] (**Figure 7**).

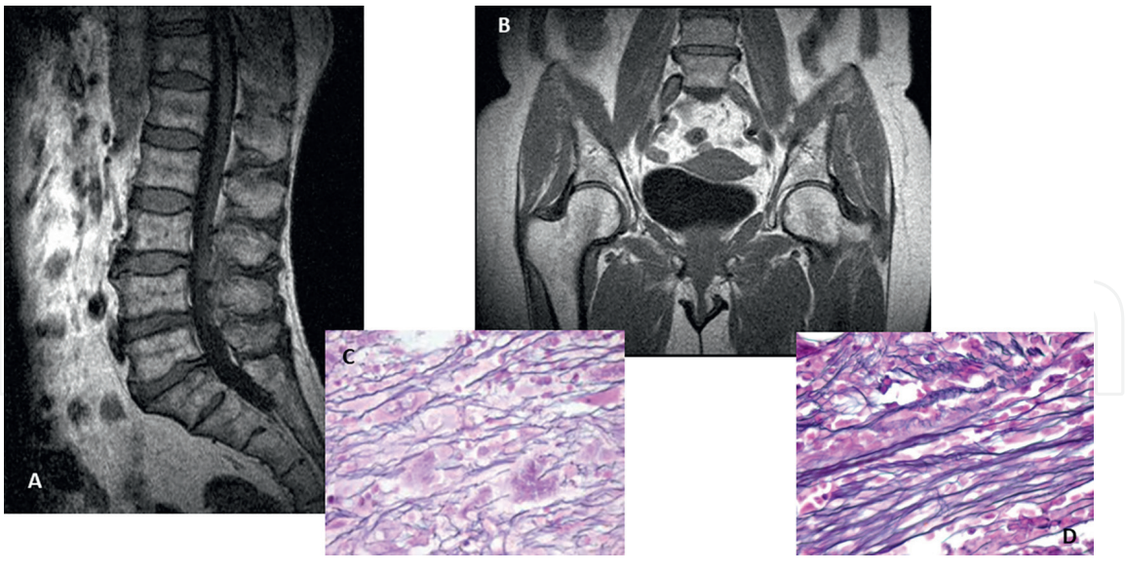

Figure 7.
Sagital spin echo (SE) T1 (A) mottled pattern, coronal SET1 (B) reticular pattern in chronic myeloproliferative neoplasia (myelofibrosis). (C) Bone marrow histological section (reticulin staining) showed reticular fibers. (D) Collagen fibers.

3.3.3.3 Systemic mastocytosis

Systemic mastocytosis is also a rare disease (less than 10% of mastocytosis), which usually affects adults and presents bone alterations in 70% of patients [26]. It has a special tropism for the axial skeleton, and although it can be silent, about 28% of patients report pain. The changes observed in simple radiology are small lytic or sclerotic lesions of focal or diffuse character (**Figure 8**). Mast cell proliferation in the

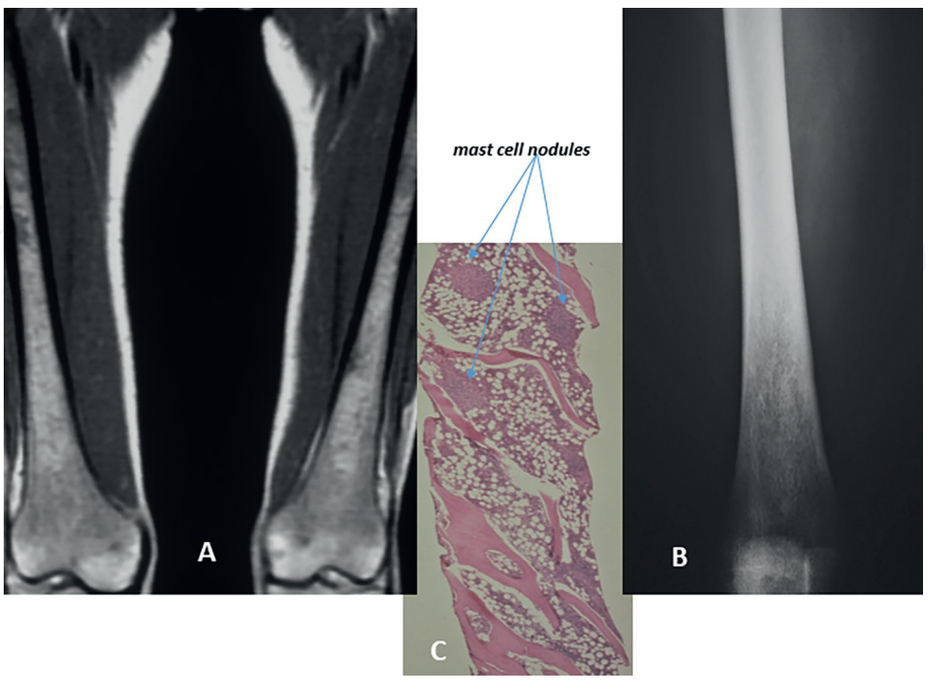

Figure 8.
Coronal spin echo (SE) T1 (A) fémurs heterogeneous reticular pattern in systemic mastocytosis. (B) Plain radiology of the femur (C). Bone marrow histological section (hematoxylin–eosin staining. HE×4). ↓ *Showed mast cell nodules.*

bone marrow stimulates fibroblastic activity with granulomatous reaction, resulting in trabecular destruction with replacement by neoformed bone. Soft tissue masses and deformities secondary to fractures may also be observed. MRI shows hypointense lesions in all sequences with diffuse distribution and homogeneous or mottled character that affect the axial skeleton and may extend to femurs and proximal humerus [30]. In any case, the infiltration presents a nonspecific signal, although sometimes it is not detectable by other diagnostic means [31].

3.3.4 Bone marrow aplasia and hypoplasia

Acquired aplasia is of unknown cause and may be secondary to chemical agents, drugs, or infectious agents. Some cases are irreversible. Biopsy is usually diagnostic, demonstrating the absence of cells or marked hypocellularity with the predominance of fatty marrow and fibrosis [32]. It should be kept in mind that areas of increased hematopoiesis may coexist with hypo- or acellular marrow, so that bone marrow biopsy from the iliac crest is a sample that does not always reflect the true state of marrow function. The marrow findings in cases of aplasia secondary to chemotherapy or irradiation may be diffuse or focal in cases of selective irradiation [33].

Hypocellular or aplastic marrow is characterized by a diffuse or mottled hyperintense pattern in T1, which corresponds to cellular replacement by fatty marrow. This signal enhancement is more appreciable in areas that normally contain red marrow remnants such as the proximal femur or vertebrae. In the appendicular skeleton, it is more difficult to appreciate this variation.

When there is a response to treatment, a heterogeneous pattern is observed in the vertebral bodies formed by hypointense foci in T1 and T2 that represent foci of hematopoiesis. MRI is a good method for assessing response to treatment [34, 35], taking into account that sometimes, these foci appear in vertebrae and are not seen in the pelvis, where the biopsy is normally performed if the patient recovers completely from his aplasia, the marrow returns to the normal appearance and distribution for his age.

The administration of erythropoiesis-stimulating factors as an adjuvant to chemotherapy treatment produces a patchy pattern in MRI showing hypointense foci in T1, which in T2 present identical or slightly increased signal, similar to hematopoietic foci in their behavior but located in areas where fatty marrow is normally present.

The depletion of medullary cellularity also occurs during ionizing irradiation at therapeutic doses. In vertebral irradiation, no signal changes are usually observed two weeks after treatment. Between the third and sixth week, most of the red marrow elements disappear, and there is central fatty infiltration in the vertebral body, or even a heterogeneous appearance pattern may be seen, resulting from the partial elimination of red marrow cellular elements. After six weeks, all patients will show hypersignal in T1. During the first year of irradiation with low doses (less than 30 Gy), there is marrow regeneration, but above 50 Gy, there is no recovery, with the MRI showing the limits between the zone of fatty infiltration and the zone of normal marrow. In case of irradiation at low doses, marrow regeneration in MRI could be confused with cellular infiltration of another type. Irradiation doses higher than 50 Gy are associated with complete replacement by fatty marrow due to irreversible marrow extinction [34].

3.3.5 Hematopoietic stem cell transplant

Knowing the normal MRI appearance of bone marrow repopulation after transplantation (BMT) is essential to be able to distinguish normal marrow repopulation from

tumor infiltration. The pretransplant MRI examination may show a normal appearance of the bone marrow in the spine and pelvis or an abnormal signal corresponding to infiltration, since the examination is performed prior to myeloablative treatment. In case of obtaining an MRI in this previous phase, a tendency to decrease signal in T1 and increase in STIR is observed, a modification that may be related to cellular necrosis and bone marrow edema induced by radiation and/or chemotherapy [35].

Until the third month after allo-TMO, no changes are observed in MRI in relation to the pretransplant examination. From the sixth month onwards, the changes are due to medullary colonization after induced aplasia, with the appearance of a heterogeneous signal alternating areas of hypo- and hyperintensity in T1 or a banded appearance. This characteristic appearance observed in the vertebral bodies corresponds to cellular hypointensity in the peripheral areas below the vertebral plats and a central zone of hyperintense fatty signal. Histologically, the peripheral zones correspond to hypercellular areas of hematopoietic repopulation, while the central zone is poorly cellular and rich in fat. The distribution depends on the vascularization system of the vertebral body [36].

In addition to assessing cellularity in BMT patients, MRI can be used to study metabolic alterations derived from cytotoxic treatment or immunological processes using QSCI (chemical shift selective imaging techniques) [37].

3.3.6 Lysosomal storage diseases. Gaucher disease

In metabolic storage diseases, MRI detects the changes produced in the bone marrow due to the combination of cellular infiltration, edema, and ischemia phenomena. Cellular infiltration causes hypointense areas in T1 and T2, starting at early stages in the vertebrae (**Table 2**) and progressing from the axial to the appendicular skeleton, affecting pelvis, hips, and lower extremities [37], with proximal predominance. The typical pattern shows homogeneous signal decrease in T1 and T2 in vertebral bodies and nonhomogeneous in proximal segments of lower extremities, with preserved epiphyses in most cases.

Vascular involvement causes infarcts, avascular necrosis, and pseudosteomyelitis or bone crises. Avascular necrosis is due to chronic infarcts produced by arteriolar occlusion following progressive cellular infiltration of the marrow and episodes of vasospasm and thrombosis. In the initial phase, the marrow is isointense, and the transition between normal and necrotic tissue is a low signal band in all sequences. Subsequently, the signal of the necrotic bone decreases and fractures appear due to cortical collapse [38].

Bone infarcts are visualized as low signal foci in all sequences of intramedullary diaphyseal location and sometimes bilateral. The bone crises that appear in 30–40% of patients with Gaucher disease are caused by acute intraosseous vascular obstruction. Due to edema, the marrow appears hypointense on T1 and hyperintense on T2. Sometimes subperiosteal hyperintensity is observed on T1 due to subacute phase hematoma or hemorrhage. Control studies show recovery of the physiological signal after the episode of bone crisis.

Gaucher disease causes alterations in the vertebrae due to increased intramedullary pressure due to cellular accumulation in the form of cortical endosteal resorption and vascular occlusive phenomena. Flat vertebrae are due to necrosis and compression fractures with the widening of the disc space.

Both enzyme replacement therapy and substrate reduction therapy cause a decrease in intramedullary lipid storage already visible in some patients after six

Disease	Infiltration pattern	Diagnostic utility	Evaluation of response to treatment
Myeloma/plasmacytoma	Diffuse or focal	+++ Identify masses Global distribution Differentiate MM from MGUS	+++
Aplasia	Diffuse or mottled hyperintense in T1	++++ Assessment of residual hematopoietic foci	++++ Pattern of medullary restocking, especially in spine
Lymphoma	Diffuse or focal	Identify biopsy-approachable masses	+++
Myeloproliferative neoplasms	Diffuse or focal in mastocytosis	+ Directed biopsy in foci suggestive of mast cell accumulation	+
BMT	Normal, focal	++ Identify pretransplant marrow infiltration	+++ Pattern of normal or tumor marrow repopulation
Lysosomal storage disease. Gaucher disease	Homogeneous or heterogeneous according to localization	++++ Essential to determining the degree of BM involvement	++++ Essential to know the response rate in BM
Osteonecrosis	Hypointensity in T1 and hyperintensity in T2 due to edema	++++	++++

Table 2.
Indications for bone marrow MRI and degree of usefulness in relation to the disease.

months, with clearance and recovery of the physiological signal in MRI, as well as the disappearance of edema in bone crises [39] (**Figure 9**). In addition, in the examination of the bone marrow by MRI, other alterations not related to Gaucher disease are detected, such as vertebral hemangiomas, discopathies, etc., which stand out for their frequency in these patients [40].

3.4 Posttreatment evaluation in hematological malignancies

The initial applications of MRI in hematology were aimed at defining the presence of lesions not detectable by other imaging procedures, the maximum exponent being the assessment of intraosseous involvement in multiple myeloma. With the incorporation of BMT, MRI acquired a new dimension for the clinician, as an instrument to define the status of the BM in patients requiring this procedure, particularly in the case of bone marrow aplasia.

MRI, due to its sensitivity in the detection of cellular infiltration, is useful in the initial phase as an assessment of the extent of the disease. This quantitative extension study will also be important, together with the rest of the tests, when considering

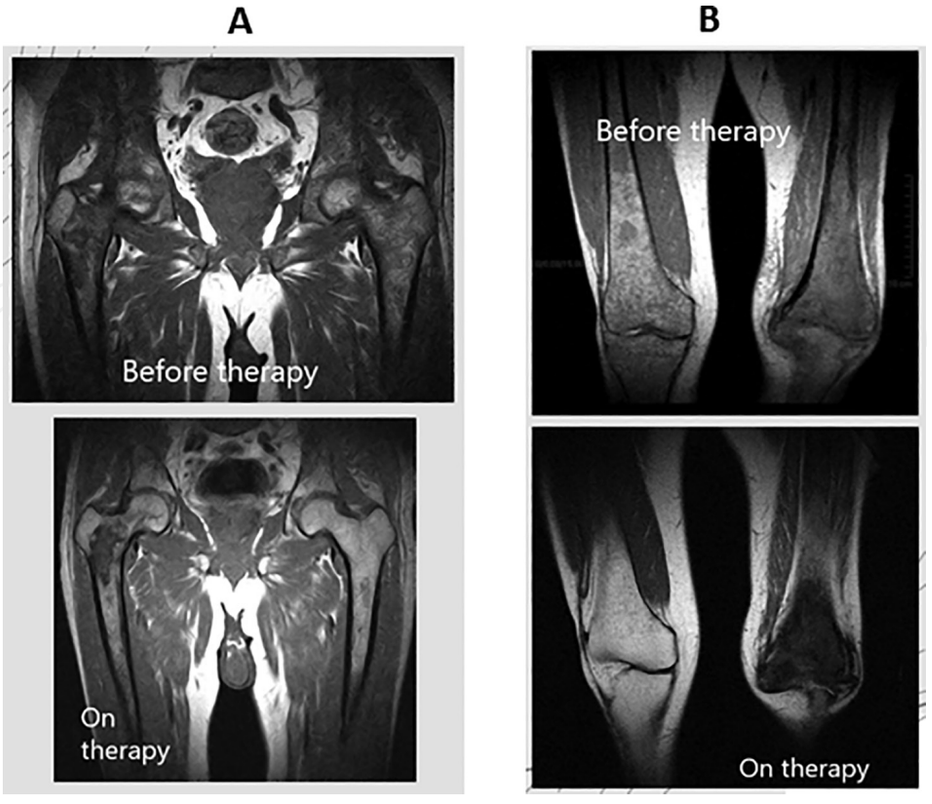

Figure 9.
Coronal spin echo (SE) T1 (A) pelvis and femurs nonhomogeneous mottled pattern with infarcts in Gaucher disease before and after therapy. The therapy causes a decrease in intramedullary lipid storage with clearance and recovery of the physiological signal. Nevertheless, complications such as infarcts or necrosis are irreversible and more visible in MRI once the infiltration has been cleared. (B) Coronal spin echo (SE) T1 femurs and tibias nonhomogeneous mottled pattern with large infarct-necrosis in Gaucher disease before and after therapy.

therapy. In the evaluation of the therapeutic response, MRI can show the degree of bone marrow involvement, being complementary to the methods that assess the progression of bone mineralization.

4. Practical considerations

MRI has proved to be a useful tool for obtaining a global map of the contents of the bone marrow cavity and the applications of the technique to the study of different processes. Assessment of bone marrow is often complex due to the presence of multiple patterns and their evolutionary change with age and disease.

Structured reports are the result of applying a logical structure to the radiological report, and the rules of elaboration comprise several criteria: (I) using a uniform language. The standardization of terminology avoids ambiguity in reporting and makes it easier to compare reports. (II) Accurately describe the radiological findings, following a prescribed order with review questions and answers. (III) Drafting using diagnostic screening tables. (IV) Respect the radiologists' workflow by facilitating the work and not hindering it [41].

The creation of structured radiological reports for the study of bone marrow is of great relevance in order to unify terms and provide the most objective assessment possible. Our group has recently published a structured report based on eight items (demographic data, diagnostic suspicion, technical data, type of exam initial or

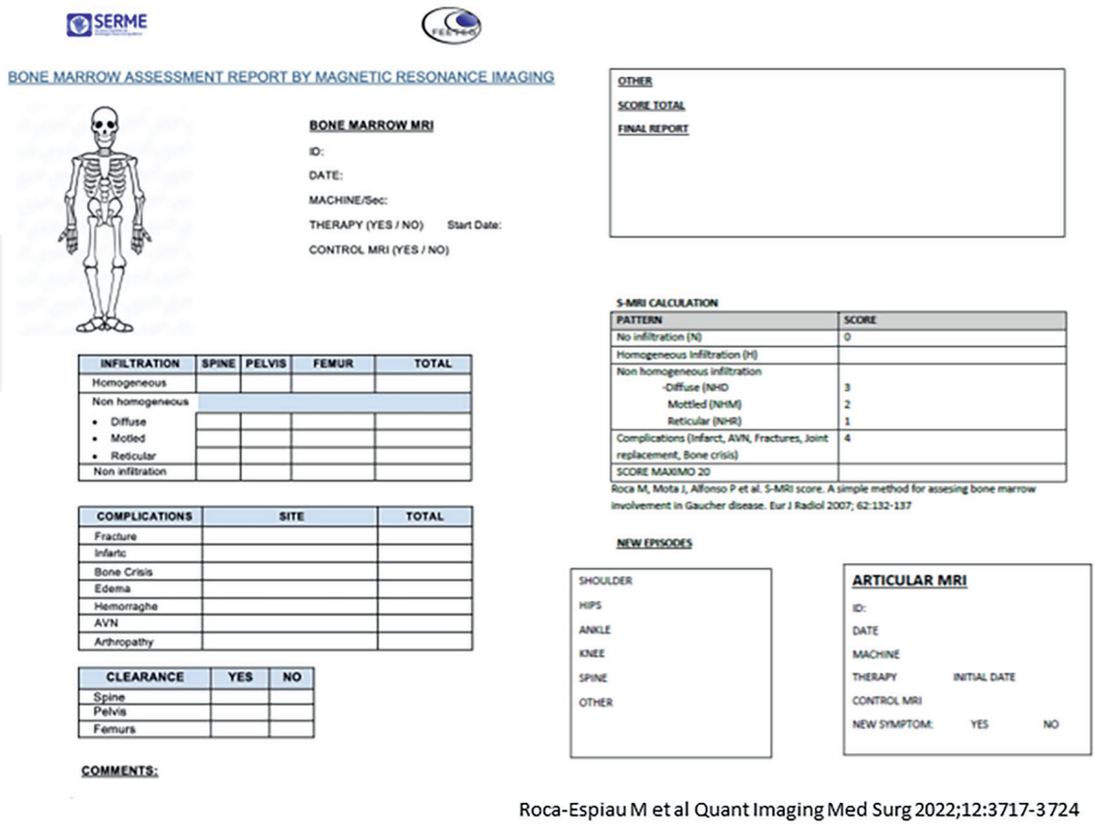
SERME

BONE MARROW ASSESSMENT REPORT BY MAGNETIC RESONANCE IMAGING

BONE MARROW MRI

ID:

DATE:

MACHINE/Sec:

THERAPY (YES / NO) Start Date:

CONTROL MRI (YES / NO)

INFILTRATION	SPINE	PELVIS	FEMUR	TOTAL
Homogeneous				
Non homogeneous				
• Diffuse				
• Motled				
• Reticular				
Non infiltration				

COMPLICATIONS	SITE	TOTAL
Fracture		
Infartc		
Bone Crisis		
Edema		
Hemorraghe		
AVN		
Arthropathy		

CLEARANCE	YES	NO
Spine		
Pelvis		
Femurs		

COMMENTS:

OTHER

SCORE TOTAL

FINAL REPORT

S-MRI CALCULATION

PATTERN	SCORE
No infiltration (N)	0
Homogeneous Infiltration (H)	
Non homogeneous infiltration	
-Diffuse (NHD	3
Mottled (NHM)	2
Reticular (NHR)	1
Complications (Infarct, AVN, Fractures, Joint replacement, Bone crisis)	4
SCORE MAXIMO 20	

Roca M, Mota J, Alfonso P et al. S-MRI score. A simple method for assesing bone marrow involvement in Gaucher disease. Eur J Radiol 2007; 62:132-137

NEW EPISODES

SHOULDER

HIPS

ANKLE

KNEE

SPINE

OTHER

ARTICULAR MRI

ID:

DATE

MACHINE

THERAPY INITIAL DATE

CONTROL MRI

NEW SYMPTOM: YES NO

Roca-Espiau M et al Quant Imaging Med Surg 2022;12:3717-3724

Figure 10.
Structured report for MRI bone marrow exam. Roca-Espiau et al. 2022.

control, patterns and involvement distribution, complications and their location, and summarized comments). It has been designed to provide guidance for radiologists when reporting protocol assessments to unified criteria, allow comparisons and decrease inter observers' variability [42] (**Figure 10**).

The structured radiological reports provide an answer in daily clinical practice, where situations of uncertainty are generated due to the lack of knowledge of the radiological semiology of the bone marrow, technical limitations in an extensive organ, and variability in the maturation of the bone marrow tissue and its pathological affectation. This involves both diagnosis and follow-up in the face of differentiated therapeutic approaches.

Nowadays, machine learning is revolutionizing the way data are analyzed in clinics and is helping to develop digital tools for diagnosis, disease progression prediction, and treatment responses. In our experience, using machine learning in rare diseases provides an opportunity to analyze agglomerated and heterogeneous data to create quality predictive models and identify risk features [43].

In the case of bone marrow diseases, these tools can be especially useful to speed the diagnosis and obtain better prognosis assessments and personalized care in our recently published work regarding the application of machine learning tools (random forest models) in a homogeneous Gaucher group of patients with different degrees of bone marrow infiltration and complications evaluated by MRI in order to identify features that can predict the risk of bone complications defined by the presence of intraosseous ischemic events (bone crisis, infarcts, avascular necrosis) during the follow-up. We have obtained the following information shown in **Figure 11**, model A includes all variables described as significant in a previously published study [43],

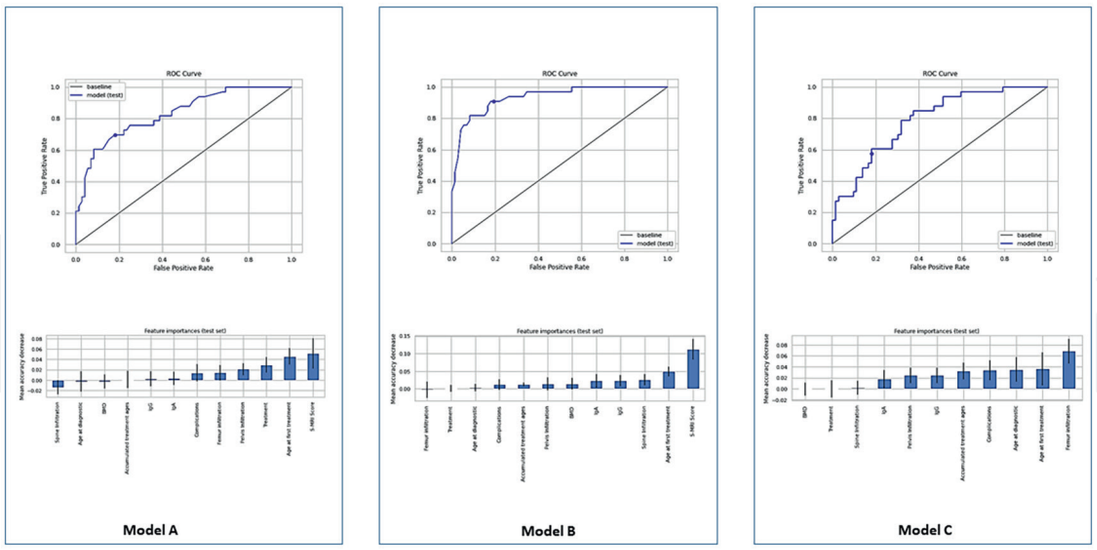

Figure 11.
ROC models. A model includes all variables. ROC B model considers whether any treatment was applied or not and features the importance of model B using the mean decrease in accuracy. ROC C model did not contain the S-MRI score and had a substantial drop in accuracy of 74.29% and an f1-score of 69.92%. The most important features for these models to predict the severity of bone affectation in Gaucher disease were the S-MRI, the age at first treatment, and the treatment used.

model B considered whether a specific treatment was applied or not, and model C ignored the degree of infiltration according to the S-MRI punctuation score [44]. The results muestran la relevancia del grado de infiltración de medulla ósea y la localización para estimar el riesgo de desarrollar complicaciones [45].

More recently, radiomics has been incorporated, which is the science of non-invasively studying features of medical images imperceptible to the human eye by applying automated algorithms to associate them with specific physiological states. Integrating clinical, biological, and therapeutic data with imaging by applying artificial intelligence methods to these studies provides a broad perspective and models that can predict the risk of complications. Today Radiomics is a science Radiomics converts medical images into mineable data by extracting quantitative characteristics [46].

The main goal is to transform imaging into actionable predictions. Programs through imaging and address healthcare issues by creating image-based predictive AI models. This outcome will allow when evaluating an MRI acquired after treatment, to assess the evolution of the patient's bone marrow involvement and to predict how they are responding to treatment. The integration of clinical, biological and/or molecular data in the classification method will be evaluated to optimize and increase its performance.

The field in which most studies are being carried out is oncology. Thanks to radiomics, diagnostic and prognostic biomarkers have been identified, associated with the development of metastases and overall patient survival in different types of cancer [47, 48].

In conclusion, in the area of bone marrow diseases, the use of machine learning provides an opportunity to analyze agglomerated and heterogeneous data to create quality predictive models and identify risk features. And it can provide important digital solutions to empower physicians to achieve health objectives [49]. Nevertheless, validation is required prior to widespread adoption in clinical practice.

Author details

Pilar Giraldo Castellano[1*] and Mercedes Roca Espiau[2]

1 Hematology, Hospital Quironsalud, FEETEG, Zaragoza, Spain

2 Radiology, FEETEG, Zaragoza, Spain

*Address all correspondence to: giraldocastellano@gmail.com

IntechOpen

References

[1] Giraldo P, Roca M, Rubio-Félix D. Resonancia magnética en enfermedades hematológicas. Madrid: Grupo Aula Médica; 2001

[2] Liu X, Faes L, Kale AU, Wagner SK, et al. A comparison of deep learning performance against health-care professionals in detecting diseases from medical imaging: A systematic review and meta-analysis. Lancet Digital Health. 2019;**1**(6):e271-e297. DOI: 10.1016/S2589-

[3] Roca M. Resonancia magnética del sistema músculo-esquelético. Barcelona: Doyma; 1992. pp. 1-23

[4] Howe BM, Johnson GB, Wenger DE. Current concepts in MRI of focal and diffuse malignancy of bone marrow. Seminars in Musculoskeletal Radiology. 2013;**17**:137-144

[5] Vande Berg BC, Malghem J, Lecouvet FE, Maldague B. Magnetic resonance imaging of normal bone marrow. European Radiology. 1998;**8**:1327-1334

[6] Lang P, Friz R, Majumdar S, Vahlensieck M, Peterfy C, Genant HK. Hematopoietic bone marrow in the adult knee: Spin-echo and opposed-phase gradient-echo MR imaging. Skeletal Radiology. 1993;**22**:95-103

[7] Vogler JB 3rd, Murphy WA. Bone marrow imaging. Radiology. 1988;**168**(3):679-693. DOI: 10.1148/radiology.168.3.3043546

[8] Moulopoulos LA, Dimopoulos MA. Magnetic resonance imaging of the bone marrow in hematologic malignancies. Blood. 1997;**90**(6):2127-2147

[9] Roca M, Giraldo P. Magnetic resonance in the diagnosis of extent and osseous complications of Gaucher's disease type 1. Radiology (Supl.). 1997;**205**:632

[10] Bernstein ZS, Kim EB, Raje N. Bone disease in multiple myeloma: Biologic and clinical implications. Cell. 2022;**11**(15):2308. DOI: 10.3390/cells11152308

[11] Moulopoulos LA, Varma DGK, Dimopoulos MA, Leeds EN, Kim EE, Johnston DA, et al. Multiple myeloma: Spinal MR imaging in patients with untreated newly diagnosed disease. Radiology. 1992;**185**:833-840

[12] Libshitz HI, Malthouse SR, CunninghamD,MacVicarAD,HusbandJE. Multiple myeloma: Appearance at MR imaging. Radiology. 1992;**182**:833-837. DOI: 10.1148/radiology.182.3.1535904

[13] Smith DB, Scarffe JH, Eddleston B. The prognostic significance of x-ray changes at presentation and reassessment in patients with multiple myeloma. Hematological Oncology. 1998;**6**:1-6

[14] Vande Berg BC, Lecouvet FE, Michaux L, Ferrant A, Maldague B, Malghem J. Magnetic resonance imaging of the bone marrow in hematological malignancies. European Radiology. 1998;**8**:1335-1344. DOI: 10.1007/s003300050548

[15] Dimopoulos MA, Moulopoulos LA, Smith T, Delasalle KB, Alexanian R. Risk for disease progression in asymptomatic multiple myeloma. The American Journal of Medicine. 1993;**94**:57

[16] Rajkumar SV, Dimopoulos MA, Palumbo A, Blade J, Merlini G,

Mateos MV, et al. International myeloma working group updated criteria for the diagnosis of multiple myeloma. The Lancet Oncology. 2014;**15**:e538-e548

[17] Mosebach J, Thierjung H, Schlemmer HP, Delorme S. Multiple myeloma guidelines and their recent updates: Implications for imaging. Rofo. 2019;**191**(11):998-1009. DOI: 10.1055/a-0897-3966

[18] Moulopoulos LA, Dimopoulos MA, Alexanian MD, Leeds EN, Libshitz HI. Multiple myeloma: MR patterns of response to treatment. Radiology. 1994;**193**:441-446

[19] Giles SL, Messiou C, Collins DJ, Morgan VA, Simpkin CJ, West S, et al. Whole-body diffusion-weighted MR imaging for assessment of treatment response in myeloma. Radiology. 2014;**271**:785-794

[20] Baur A, Stabler A, Lamerz R, Bartl R, Reiser M. Light chain deposition disease in multiple myeloma: MR imaging features correlated with histopathological findings. Skeletal Radiology. 1988;**27**:173-176

[21] Holland J, Trenkner DA, WassermanTH.Plasmacytoma:Treatment results and conversion to myeloma. Cancer. 1992;**69**:1513

[22] Dimopoulos M, Kyle R, Fermand JP, Rajkumar SV, San Miguel J, Chanan-Khan A, et al. International myeloma workshop consensus panel 3 - consensus recommendations for standard investigative workup: Report of the international myeloma workshop consensus panel 3. Blood. 2011;**117**:4701-4705

[23] Sanz L, Cervantes F, Mercader JM, Rozman M, Rozman C, Montserrat E. Afección oculta de la médula ósea en la enfermedad de Hodgkin: detección por resonancia magnética. Medicina Clínica. 1996;**107**:143-145

[24] Smith R, Schilder K, Shaer A, Negendak W. Lymphoma staging with bone marrow MRI. American Society of Clinical Oncology. 1995;**14**:390

[25] Albano D, Patti C, Lagalla R, Midiri M, Galia M. Whole-body MRI, FDG-PET/CT, and bone marrow biopsy, for the assessment of bone marrow involvement in patients with newly diagnosed lymphoma. Journal of Magnetic Resonance Imaging. 2017;**45**:1082-1089

[26] Resnick D, Haghighi P. Myeloproliferative disorders. In: Resnick D, editor. Diagnosis of Bone and Joint Disorders. 2.ª ed. Vol. 4. Philadelphia: Saunders; 1996

[27] Slot S, van de Donk NWCJ, Otten RHJ, Boden BJH, Zijlstra J, Raijmakers PGHM, et al. The value of bone marrow, liver, and spleen imaging in diagnosis, prognostication, and follow-up monitoring of myeloproliferative neoplasms: A systematic review. Cancer Imaging. 2021;**21**:36. DOI: 10.1186/s40644-021-00405-7

[28] Luker GD, Nguyen HM, Hoff BA, Galbán CJ, Hernando D, Chenevert TL, et al. A pilot study of quantitative MRI parametric response mapping of bone marrow fat for treatment assessment in Myelofibrosis. Tomography. 2016;**2**:67-78. DOI: 10.18383/j.tom. 2016.00115

[29] Giraldo-Castellano P, Roca-Espiau M. Exploraciones de imagen (II). In: Hernandez- Nieto L, editor. Biopsia de la médula ósea. Perspectiva clínico-patológica . 2ª ed. Madrid. 2017. pp. 193. ISBN: 978-84-697-6855-6

[30] Avila NA, Ling A, Metcalfe DD, Worobec AS. Mastocytosis: Magnetic

resonance imaging patterns of marrow disease. Skeletal Radiology. 1998;**27**:119-126

[31] Roca M, Mota J, Giraldo P, García Erce JA. Systemic mastocytosis: MRI of bone marrow involvement. European Radiology. 1999;**9**:1094-1097

[32] Marsh JC. Bone marrow failure syndromes. Clinical Medicine (London, England). 2005;**5**(4):332-336. DOI: 10.7861/clinmedicine.5-4-332

[33] Kaplan PA, Asleson RJ, Klassnen LW, Dugan MJ. Bone marrow patterns in aplastic anemia: Observations with 1.5 T MR imaging. Radiology. 1987;**164**:441-444

[34] Yang X, Bai Y, Guo H, Shi M, Zhang W, Pei Y, et al. Evaluating and monitoring bone marrow hypoplasia in adults with aplastic anemia via high-resolution iliac magnetic resonance imaging in the current era. Medicine (Baltimore). 2019;**98**(49):e18214. DOI: 10.1097/MD.0000000000018214

[35] Schick F, Einsele H, Weiss B, Jung WI, Lutz O, Claussen CD. Characterization of bone marrow after transplantation by means of magnetic resonance. Annals of Hematology. 1995;**70**:3-13. DOI: 10.1007/BF01715375

[36] Schick F, Einsele H, Weiss B, Forster J, Lutz O, Kanz L, et al. Assessment of the composition of bone marrow prior to and following autologous BMT and PBSCT by magnetic resonance. Annals of Hematology. 1996;**72**:361-370. DOI: 10.1007/s002770050187

[37] Maas M, Van Kuijk C, Stoker J, Hollak CE, Akkerman EM, Aerts JF, et al. Quantification of bone involvement in Gaucher disease: MR imaging bone marrow burden score as an alternative to Dixon quantitative chemical shift MR imaging-initial experience. Radiology. 2003;**229**:554-561

[38] Marcucci G, Zimran A, Bembi B, Kanis J, Reginster JY, Rizzoli R, et al. Gaucher disease and bone manifestations. Calcified Tissue International. 2014;**95**:477-494. DOI: 10.1007/s00223-014-9923-y

[39] Mariani G, Perri M, Minichilli F, Ortori S, Linari S, Giona F, et al. Standardization of MRI and Scintigraphic scores for assessing the severity of bone marrow involvement in adult patients with type 1 Gaucher disease. AJR. American Journal of Roentgenology. 2016;**206**:1245-1252. DOI: 10.2214/AJR.15.15294

[40] Andrade M, Valero E, Roca M, Giraldo P. The utility of magnetic resonance imaging for bone involvement in Gaucher disease. Assessing more than bone crises. Blood Cells, Molecules & Diseases. 2016;**pii: S1079-9796**(16):30219-30214

[41] Nobel JM, van Geel K, Robben SGF. Structured reporting in radiology: A systematic review to explore its potential. European Radiology. 2022;**32**:2837-2854. DOI: 10.1007/s00330-021-08327-5

[42] Roca-Espiau M, Valero-Tena E, Ereño-Ealo MJ, Giraldo P. Structured bone marrow report as an assessment tool in patients with hematopoietic disorders. Quantitative Imaging in Medicine and Surgery. 2022;**12**:3717-3724. DOI: 10.21037/qims-21-1191

[43] Andrade-Campos MM, de Frutos LL, Cebolla JJ, Serrano-Gonzalo I, Medrano-Engay B, Roca-Espiau M, et al. Identification of risk features for complication in Gaucher's disease patients: A machine learning analysis of the Spanish registry of Gaucher

disease. Orphanet Journal of Rare Diseases. 2020;**15**(1):256. DOI: 10.1186/s13023-020-01520-7

[44] Roca M, Mota J, Alfonso P, Pocoví M, Giraldo P. S-MRI score: A simple method for assessing bone marrow involvement in Gaucher disease. European Journal of Radiology. 2007;**62**:132-137. DOI: 10.1016/j.ejrad.2006.11.024

[45] Valero-Tena E, Roca-Espiau M, Verdú-Díaz J, Diaz-Manera J, Andrade-Campos M, Giraldo P. Advantages of digital technology in the assessment of bone marrow involvement in Gaucher's disease. Frontiers in Medicine (Lausanne). 12 May 2023;**10-18**:1098472. DOI: 10.3389/fmed.2023.1098472

[46] Lambin P, Leijenaar RTH, Deist TM, et al. Radiomics: The bridge between medical imaging and personalized medicine. Nature Reviews Clinical Oncology. 2017;**14**(12):749-762. DOI: 10.1038/nrclinonc.2017.141

[47] Avanzo M, Wei L, Stancanello J, Vallières M, Rao A, Morin O, et al. Machine and deep learning methods for radiomics. Medical Physics. Jun 2020;**47**(5):e185-e202. DOI: 10.1002/mp.13678.

[48] Faghani S, Baffour FI, Ringler MD, Hamilton-Cave M, Rouzrokh P, Moassefi M, et al. A deep learning algorithm for detecting lytic bone lesions of multiple myeloma on CT. Skeletal Radiology. 2023;**52**(1):91-98. DOI: 10.1007/s00256-022-04160-z

[49] Jandoo T. WHO guidance for digital health: What it means for researchers. Digital Health. 2020;**6**:2055207619898984